Experimental Acoustic Ground Cloak in Air

Bogdan-Ioan Popa,* Lucian Zigoneanu, and Steven A. Cummer†

Department of Electrical and Computer Engineering, Duke University, Durham, North Carolina 27708, USA

(Received 5 May 2011; revised manuscript received 14 June 2011; published 22 June 2011)

We present the design, fabrication, and performance analysis for a class of two-dimensional acoustic cloaking coatings in air. Our approach takes advantage of transformation acoustics and linear coordinate transformations that result in shells which are homogeneous, broadband, and compact. The required material parameters are highly anisotropic; however, we show that they are easily achievable in practice in metamaterials made of perforated plastic plates. The good performance of the fabricated design is assessed from measurements of the sound field produced around the cloak by a broadband source. The remarkably low complexity of the device made of perforated plastic plates shows that sound in air can be fully and effectively manipulated using realizable transformation acoustics devices.

DOI: 10.1103/PhysRevLett.106.253901 PACS numbers: 41.20.Jb, 46.40.Cd

Transformation acoustics [1–6] is a coordinate-transformation-based technique that allows unprecedented control over the propagation of acoustic waves in fluidlike materials. One of the most analyzed applications enabled by the improved control is the so-called invisibility cloak [7,8], a scattering reducing coating that applied to arbitrary objects significantly reduces their acoustic signature, and, thus, makes them hard to detect acoustically. Transformation acoustics provides the material parameters inside the coatings; however, realizing these parameters has proven to be challenging in practice. The main difficulty encountered is that such designs tend to be inhomogeneous—i.e., the parameters vary continuously with position—and very anisotropic. The complexity of the design process and resulting physical device is emphasized in a recent experimental realization of a full cloak in water [9].

Here we focus on the realization of a different class of cloaking shells labeled "carpet" or "ground cloaks" able to hide objects positioned on reflecting surfaces. Initially proposed in the context of electromagnetics [10], these devices received significant attention. It has been shown that isotropic materials can be used to implement these coatings and this property has been used to demonstrate the concept experimentally for electromagnetics [11,12]. A drawback of this quasiconformal method is that it specifies a device where the cloaking shell is many times the volume of the hidden object.

If isotropy is desirable in electromagnetics, it is not necessarily the case in acoustics, as it has been shown that broadband anisotropic acoustic composites of desired properties can be relatively easy to obtain [13–18]. As pointed out in the past in the context of electromagnetics [19,20], anisotropy allows for ground cloaks that are simultaneously homogeneous, broadband, and compact. This path has been taken to fabricate homogeneous cloaking shells working in the optical domain and made either of layers of silicon gratings [21] or, for a more limited functionality, birefringent crystals [22,23].

We showed in numerical simulations of a realizable structure made of basic materials such as steel and metal foams [24] that this approach is especially suitable for transformation acoustics based cloaks in a water host. Some of the effective parameters inside the device (mass density pseudotensor [25] and bulk modulus) that are prescribed by transformation acoustics had to be smaller than those of water, which meant that the device had to be implemented using materials less dense and more compressible than water such as metal foams.

If cloaking in air is required, however, then this method is not applicable, simply because there are, currently, no basic materials less dense and more compressible than air and, at the same time, durable enough to be practical and easy to machine to the desired shapes. In this Letter, we demonstrate a path that can be taken to overcome this difficulty, and illustrate it by designing, fabricating, and experimentally characterizing a ground cloak in air. The resulting device designed for two-dimensional (2D) applications has surprisingly low complexity being made of planar perforated plastic plates. Its good performance is assessed experimentally inside a parallel plate waveguide from measurements of the acoustic field distribution around the cloak. The structure is excited by a sound pulse short in time, thus, broadband in frequency.

Consider the dark triangular object shown in Fig. 1 placed in air on a rigid ground plane. In order to make it invisible from sound detection, we cover it with a light colored coating whose material properties are specified by the transformation acoustic theory. The advantage of this geometry is that it enables linear transformations that translate into a homogeneous cloaking material [20]. More specifically, if we map the triangular shape of the region we wish to hide in the real space (xyz coordinates) into an infinitely thin triangle that is indistinguishable from the ground plane in the virtual space (uvw coordinates), then the mapping assumes the form

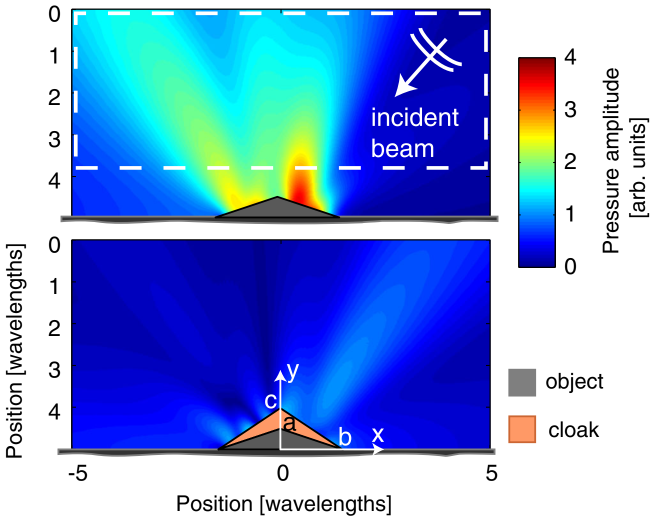

FIG. 1 (color online). Simulated acoustic signatures of triangular object (top) and object covered by cloak (bottom) placed on a reflecting horizontal surface. The signature is computed as the difference between the pressure fields with and without the target. The cloak is characterized by the realizable material parameters given by Eq. (3). The dashed rectangle surrounds the region in which we will experimentally measure the pressure fields.

$$u = x, \qquad v = \frac{c}{c-a}\left(-a + \frac{a}{b}|x| + y\right), \qquad w = w_z z, \tag{1}$$

where a, b, and c quantify the geometry. Unlike the other aforementioned designs that use similar linear transformations, we use the constant w_z as a degree of freedom that allows us to trade a slight decrease in performance for fabrication simplicity.

According to transformation acoustics [1,2,6], the material parameters inside the coating, i.e., mass density pseudotensor and bulk modulus, are given by $\boldsymbol{\rho} = \det(A)(A^{-1})^T A^{-1}\rho_0$, $B = \det(A)B_0$, where $\rho_0 = 1.29\ \mathrm{kg/m^3}$ and $B_0 = 0.15$ MPa are the parameters of air, and A is the transformation Jacobian: $A = \frac{\partial(x,y,z)}{\partial(u,v,w)} = [\frac{\partial(u,v,w)}{\partial(x,y,z)}]^{-1}$.

The principal axis components of these parameters, i.e., the material parameters that will be realized later using acoustic metamaterials, are given by

$$\begin{aligned} \rho_{11}^{\mathrm{pr}} &= w_z^{-1}(F + \sqrt{F^2 - 1})\rho_0, \\ \rho_{22}^{\mathrm{pr}} &= w_z^{-1}(F - \sqrt{F^2 - 1})\rho_0, \\ B^{\mathrm{pr}} &= w_z^{-1}\frac{c-a}{c}B_0, \end{aligned} \tag{2}$$

where ρ_{11}^{pr} and ρ_{22}^{pr} are the in-plane diagonal components of the principal axis mass density pseudotensor, and $F = 1 + a^2(b^2 + c^2)/[2b^2c(c-a)]$.

Equation (2) gives the material parameters inside the cloak, while $\alpha = \mathrm{sgn}(x)\arcsin(G/\sqrt{1+G^2})$ where $G = (b/c)[1 - (c/a - 1)(F - 1 - \sqrt{F^2 - 1})]$ gives the angle by which the xyz frame is rotated around the out-of-plane axis z in order to obtain the principal axis.

Equation (2) shows the advantage of using the out-of-plane transformation parameter w_z. If the out-of-plane direction is not transformed, i.e., $w_z = 1$, the mass density components have to satisfy $\rho_{11}^{\mathrm{pr}}\rho_{22}^{\mathrm{pr}} = \rho_0^2$ and one density component has to be less than the density of the background fluid. At the same time $B < B_0$. Since we are interested in broadband solutions, these constraints suggest that the metamaterial needed to mimic these parameters has to contain at least one basic material that is less dense and rigid than the background fluid. However, it is difficult to find such a material when the background fluid is air.

This issue is resolved by using the w_z constant that scales all material parameters in the same direction, and, consequently, can be used to bring them above those of air.

The next question is how much impact the nonunity w_z has on the cloaking performance. We notice that the wave velocity in the coating shell keeps the desired value regardless of our choice of w_z, since both $v_{ii} \equiv \sqrt{B^{\mathrm{pr}}/\rho_{ii}^{\mathrm{pr}}}$ with $i \in \{1, 2\}$ are independent of w_z. The impedance, on the other hand, is scaled by the factor w_z, since $Z_{ii} \equiv \sqrt{B^{\mathrm{pr}}\rho_{ii}^{\mathrm{pr}}} \sim w_z^{-1}$; therefore, the cloak will be slightly unmatched to the background..

To quantify the performance loss induced by $w_z \neq 1$ we consider the following example. We choose $a = 5.6$ cm, $b = 16.8$ cm, and $c = 11.2$ cm; therefore, the volume ratio object to cloak is unity. The obliquely incident pressure field symbolized by the arrow in Fig. 1 (top) is a Gaussian beam of relatively large spatial extent that models the close to cylindrical waves emitted by a regular speaker. Figure 1 (top) shows the acoustic signature of the object at 3 kHz computed as the amplitude of the difference between the sound fields obtained with and without the object placed on the reflecting surface. We notice two directions of strong scattering at approximately 45° and 90° with respect to the horizontal.

Figure 1 (bottom) shows the acoustic signature of the object covered by a cloak for which we choose $w_z^{-1} = 2.5$ in order to obtain from Eq. (2) the following easier to realize material parameters:

$$\rho_{11}^{\mathrm{pr}} = 5.7\rho_0, \quad \rho_{22}^{\mathrm{pr}} = 1.1\rho_0, \quad B^{\mathrm{pr}} = 1.25B_0, \quad \alpha = 66.9°. \tag{3}$$

Despite this value of w_z^{-1}, the cloak performance remains close to ideal, and the scattering from the object is significantly reduced. This is the behavior we wish to obtain experimentally.

Unlike electromagnetics, in acoustics it is considerably easier to fabricate an anisotropic metamaterial characterized by the effective material parameters given by Eq. (3). For our purpose we use a metamaterial made of planar

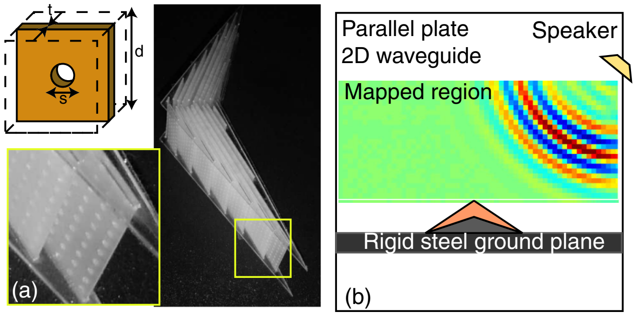

FIG. 2 (color online). Experimental setup: (a) Picture of cloak covering the object. The angle made by the perforated plastic plates with the vertical is given by Eq. (3). Inset: unit cell ($d = 5$ mm; $s = 1.6$ mm; $t = 1$ mm). (b) Two-dimensional parallel plate waveguide used to map the acoustic field around the cloak. The mapped region is highlighted together with the pulse produced by the source.

perforated plastic plates [14,15,18]. The unit cell that generates this structure is shown in the inset of Fig. 2(a).

The size and shape of the perforation determines the momentum in the rigid plate produced by a wave propagating perpendicular on the plate [14], and, therefore, can be used to control the corresponding mass density component seen by this wave [15]. This property is used to obtain the higher density component in Eq. (3). If, on the other hand, the wave propagates parallel to the plate, it will have a very small influence on it, and consequently the wave will see a density close to that of the background fluid. The compressibility of the cell, quantified by the second effective parameter, the bulk modulus, is controlled by the fractional volume occupied by the plastic plate [15,26].

The above qualitative analysis together with the numerical method presented in Ref. [15] allows us to design the dimensions of the cell components that give the desired parameters of Eq. (3). We chose a cell size of 5 mm that makes the cell at least 20 times smaller than the wavelength for frequencies between 0 and 3 kHz. The thickness of the plastic plate is 1 mm, while the perforation diameter is 1.6 mm. For this cell geometry the effective material parameters are $\rho_{11} = 5.6\rho_0$, $\rho_{22} = 1.23\rho_0$, and $B = 1.22B_0$; i.e., they are within 10% of the ideal values.

Figure 2(a) shows the fabricated cloaking device. The composing perforated plates are at the 66.9° angle given by Eq. (3), and held in place by 1 mm thick top and bottom plastic plates. The plates are aligned at the imaginary line that separates the right and left halves of the structure.

The device behavior is measured inside the 2D parallel plate waveguide sketched in Fig. 2(b). The reflecting ground plane consists of a block of steel that, similar to the cloaking shell, fills the entire height of the waveguide. An omnidirectional speaker that produces close to cylindrical sound pulses is used to excite the waveguide, as illustrated in the figure. Each pulse is a time domain Gaussian modulated by a $f_0 = 3$ kHz sinusoidal signal, so that its frequency spectrum has a Gaussian shape centered at f_0 whose 3 dB band is approximately $f_0/3 = 1$ kHz. The sound distribution around the object is measured by a microphone moved in steps of 2 cm in the region directly above the object and cloak marked in Fig. 2(b).

Figure 3 shows the reflected fields measured with the ground plane by itself (left panels), with the object placed on top of the ground plane (middle panels), and finally with the object covered by the cloak (right panels). The top and bottom panels show the measured sound waves as they propagate during a 880 μs time interval.

We notice the acoustic signature of the bare object (middle panels), namely, the shadow in the middle of the scattered wave front and the strong reflection in the vertical direction, in agreement with the numerical simulations. This acoustic signature is canceled when the cloaking coating covers the object (right panels). Apart from a small attenuation, the shape of the wave front in the latter case is identical to the ideal front (left panels), a testament of the fact that the wave phase velocity inside the cloak assumes the theoretically predicted value. In contrast, the bare

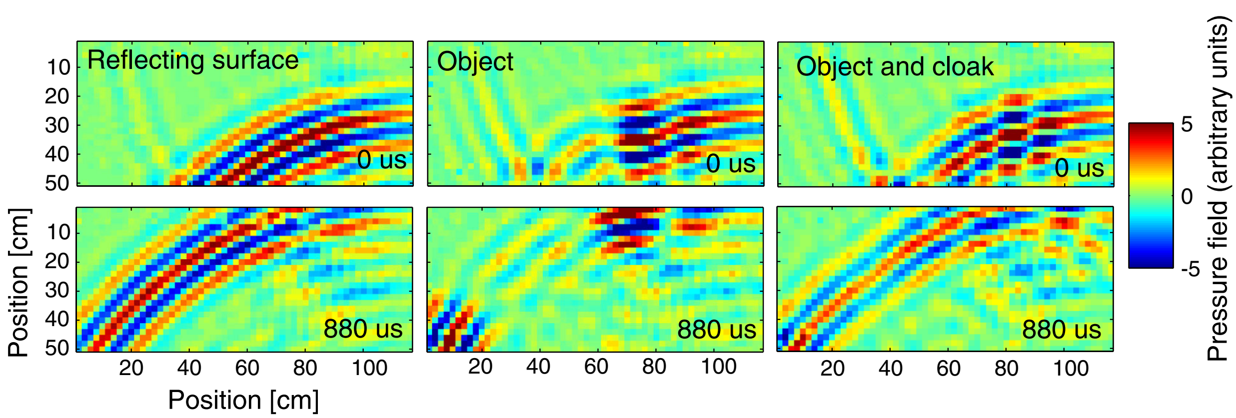

FIG. 3 (color online). Measured scattered fields. Left panels: specular reflection from the ground plane. Middle panels: pressure field scattered by the object placed on the ground plane. Right panels: scattering from the object covered by cloak. Bottom panels represent wave forms measured 880 μs after the measurements shown in the top panels.

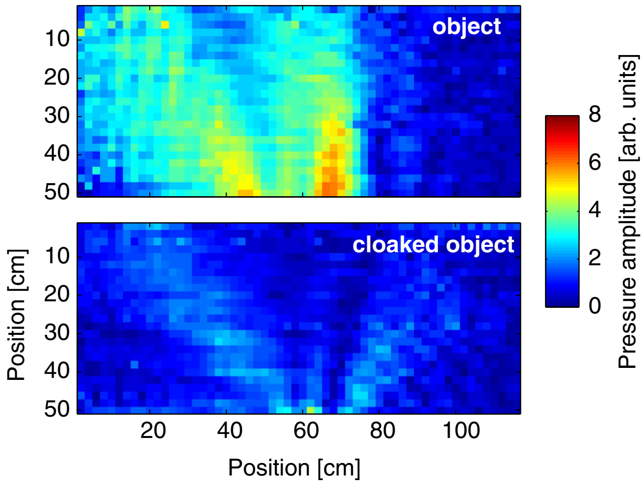

FIG. 4 (color online). Measured acoustic signature of object covered by cloak (bottom) is significantly reduced when compared with the acoustic signature of the object (top) in agreement with the theoretical prediction of Fig. 1. The signature of each target is computed as the difference between the fields with and without the target.

object causes a large phase advance in the middle of the pulse where the amplitude is smaller.

After passing through the cloak, the pulse keeps its time domain Gaussian shape, which demonstrates the broadband nature of the device. Similar measurements (not shown) in which the incident signal was centered at 1.5 kHz further confirm this observation.

The time domain measurements are Fourier transformed in order to obtain (see Fig. 4) the frequency domain acoustic signature of the object (top) and object covered by cloak (bottom) at 3 kHz. The cloak cancels both directions of strong scattering that correspond to the shadow and strong vertical reflections, in very good agreement with the theoretical predictions of Fig. 1.

The fabricated cloak induces an additional direction of slight scattering when compared with the theoretical behavior caused by slight losses in the fabricated cloak that are not taken into account in the earlier numerical simulation. Additional simulations showed, however, that, if we model losses as a small imaginary part of the bulk modulus, the measured field distribution is consistent with a bulk modulus of $B = (1.24 + j0.15)B_0$, with $j \equiv \sqrt{-1}$. The otherwise excellent match between the simulation and experiment (see Figs. 1 and 4) demonstrates the effectiveness of the design method.

To conclude, we demonstrated a procedure to obtain acoustic cloaking devices and showed its effectiveness experimentally. Our cloaking device is made of easy to obtain planar, perforated plastic plates. The device performance is assessed from acoustic field measurements performed inside an acoustic parallel plate waveguide. These measurements confirm the expected behavior obtained in numerical simulations and demonstrate the effectiveness of the design method.

*bap7@ee.duke.edu
†cummer@ee.duke.edu

[1] S. A. Cummer and D. Schurig, New J. Phys. **9**, 45 (2007).
[2] H. Chen and C. T. Chan, Appl. Phys. Lett. **91**, 183 518 (2007).
[3] S. A. Cummer, B. I. Popa, D. Schurig, D. R. Smith, J. B. Pendry, M. Rahm, and A. F. Starr, Phys. Rev. Lett. **100**, 024301 (2008).
[4] D. Torrent and J. Sanchez-Dehesa, New J. Phys. **10**, 063 015 (2008).
[5] Y. Cheng, F. Yang, J. Y. Xu, and X. J. Liua, Appl. Phys. Lett. **92**, 151 913 (2008).
[6] A. N. Norris, Proc. R. Soc. A **464**, 2411 (2008).
[7] J. B. Pendry, D. Schurig, and D. R. Smith, Science **312**, 1780 (2006).
[8] U. Leonhardt, Science **312**, 1777 (2006).
[9] S. Zhang, C. Xia, and N. Fang, Phys. Rev. Lett. **106**, 024301 (2011).
[10] J. Li and J. B. Pendry, Phys. Rev. Lett. **101**, 203901 (2008).
[11] R. Liu, C. Ji, J. J. Mock, J. Y. Chin, T. J. Cui, and D. R. Smith, Science **323**, 366 (2009).
[12] J. Valentine, J. Li, T. Zentgraf, G. Bartal, and X. Zhang, Nature Mater. **8**, 568 (2009).
[13] G. W. Milton, M. Briane, and J. R. Willis, New J. Phys. **8**, 248 (2006).
[14] J. B. Pendry and J. Li, New J. Phys. **10**, 115 032 (2008).
[15] B.-I. Popa and S. A. Cummer, Phys. Rev. B **80**, 174303 (2009).
[16] D. Torrent and J. Sanchez-Dehesa, Phys. Rev. Lett. **105**, 174301 (2010).
[17] J. Li, L. Fok, X. Yim, G. Bartal, and X. Zhang, Nature Mater. **8**, 931 (2009).
[18] L. Zigoneanu, B.-I. Popa, and S. A. Cummer, J. Appl. Phys. **109**, 054 906 (2011).
[19] Y. Luo, J. Zhang, H. Chen, L. Ran, B.-I. Wu, and J. Au. Kong, IEEE Trans. Antennas Propag. **57**, 3926 (2009).
[20] W. Zhu, C. Ding, and X. Zhao, Appl. Phys. Lett. **97**, 131 902 (2010).
[21] J. Zhang, L. Liu, Y. Luo, S. Zhang, and N. A. Mortensen, Opt. Express **19**, 8625 (2011).
[22] X. Chen, Y. Luo, J. Zhang, K. Jiang, J. B. Pendry, and S. Zhang, Nature Commun. **2**, 176 (2011).
[23] B. Zhang, Y. Luo, X. Liu, and G. Barbastathis, Phys. Rev. Lett. **106**, 033901 (2011).
[24] B.-I. Popa and S. A. Cummer, Phys. Rev. B (to be published).
[25] J. R. Willis, Int. J. Solids Struct. **21**, 805 (1985).
[26] A. B. Wood, *A Textbook of Sound; Being an Account of the Physics of Vibrations with Special Reference to Recent Theoretical and Technical Developments* (Macmillan, New York, 1955).